Bypass transition in compressible boundary layers

Pedro Paredes, Meelan Choudhari, Fei Li & Chau-Lyan Chang

Computational AeroSciences Branch
NASA Langley Research Center

6^{th} Symp. on Global Flow Instability and Control
Sep 28 - Oct 2, 2015, Hersonissos, Crete, GR

Paths to transition[1]: The rule of transient growth

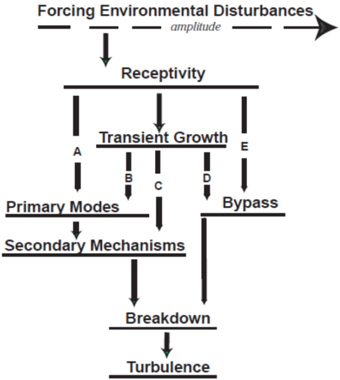

- The non-normality of the NS equations can give rise to transient energy amplification

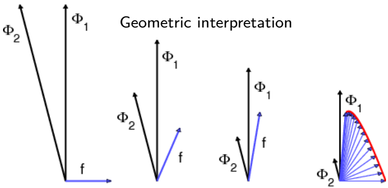

- Transient growth is a candidate mechanism for several cases of *bypass transition* wherein the route to laminar-turbulent transition *bypasses* the well-known paths to turbulence via modal instabilities of the underlying laminar basic state, for example:
  - large bluntness cones,
  - spherical forebodies, ...

[1] M.V. Morkovin, E. Reshotko, and T. Herbert. "Transition in open flow systems - A reassessment". In: *Bull. Am. Phys. Soc.* 39:1882 (1994).

Large bluntness cones[2]

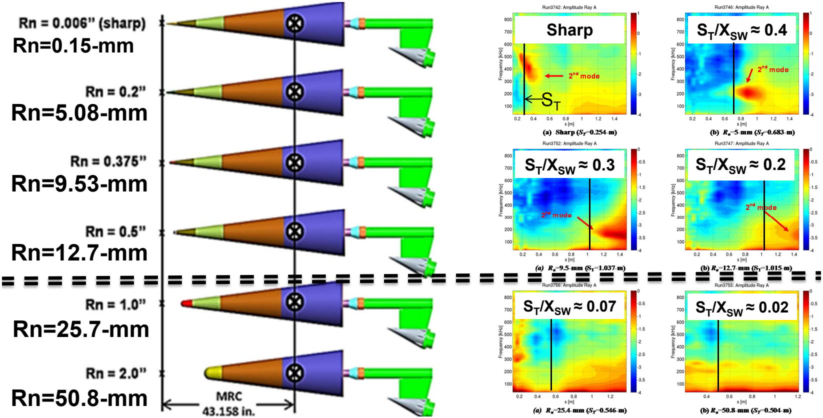

- Small blutness: the transition front moves back relative to sharp cone.
- Large blutness: the transition front moves forward. **Why?**

[2] E.C. Marineau et al. *Mach 10 boundary-layer transition experiments on sharp and blunted cones*. AIAA Paper 2014-3108. 2014.

Spherical forebodies: the blunt body paradox[3,4]

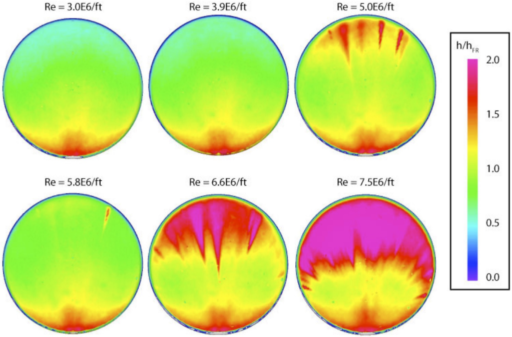

Figure 14. CEV Global Heating Distribution from Test 6944, α = 28-deg, 8-in. diam. model

- Transition observed while the flow is T-S stable, Görtler stable (convex curvature) and crossflow is negligible. **Why?**

---

[2] Note that images for Re=5.0E6/ft and Re=5.8E6/ft are interchanged.

[3] E. Reshotko and A. Tumin. "The blunt body paradox - A case for transient growth". In: *Proc. of the IUTAM Laminar-Turbulent Symposium V*. ed. by H. Fasel and W. Saric. Sedona, AZ, USA, 2000, p. 403.

[4] B.R. Hollis. *Blunt-body entry vhicle aerothermodynamics: transition and turbulence on the CEV and MSL configurations*. AIAA Paper 2010-4984. 2010.

Can TG theory explain transition in these cases?[7]

- Reshotko and Tumin[5] suggested transient growth as a possible explanation for transition over blunt nose tips and showed that a transition criterion based on linear optimal growth provided successful correlation with the PANT database ($M \leq 6$).
- Recent data[6] corresponds to higher Mach numbers ($M \geq 6$).

Current ongoing work:

- supersonic and hypersonic Mach numbers
- nonlinear effects (nonlinear streak development, streak instabilities, interaction with boundary layer instabilities, ...)
- spatial approach including non-parallel effects
- realistic geometries

[5] E. Reshotko and A. Tumin. "Role of Transient Growth in Roughness-Induced Transition". In: *AIAA J.* 42 (2004), pp. 766–770.

[6] E.C. Marineau et al. *Mach 10 boundary-layer transition experiments on sharp and blunted cones*. AIAA Paper 2014-3108. 2014.

[7] P. Paredes et al. *Transient growth analysis of compressible boundary layers with parabolized stability equations*. (Submitted to SciTech 2016). 2016.

Zero-pressure-gradient flat plate BL at Mach 3

- Linear optimal disturbances
  - Verification against prior results using self-similar base flow solution
  - Extension to N-S base flow solution including leading edge shock
- Non-linear evolution of finite-amplitude linearly optimal disturbances
- Instability analysis of the perturbed flow

- Examples of supersonic/hypersonic vehicles with *flat plate* components:

- BOEING X-51A (Mach 5)[8]

- NASA X-43A (Mach 10)[9]

[8] http://www.wpafb.af.mil/news/story.asp?id=123346970

[9] http://www.nasa.gov/missions/research/x43-main.html

Transient growth analysis using PSE[10]

- The optimal initial disturbance, $\tilde{\mathbf{q}}_0$, is defined as the inflow condition at x_0 that leads to maximum energy amplification or gain, G, up to a specified position, x_1.
- Objective function: $J(\tilde{\mathbf{q}}) = G = \frac{E(x_1)}{E(x_0)}$.
- Mack's energy norm: $E(\xi) = \int_\Omega \tilde{\mathbf{q}}(x)^H \mathbf{M} \tilde{\mathbf{q}}(x)\,\mathrm{d}\Omega$, with

$$\mathbf{M} = \mathrm{diag}\left[\frac{\bar{T}(x)}{\gamma\bar{\rho}(x)M^2}, \bar{\rho}(x), \bar{\rho}(x), \bar{\rho}(x), \frac{\bar{\rho}(x)}{\gamma(\gamma-1)\,\bar{T}(x)M^2}\right].$$

- Variational formulation using direct and adjoint PSE,

$$\mathcal{L}(\tilde{\mathbf{q}}, \tilde{\mathbf{q}}^*) = J(\tilde{\mathbf{q}}) - \langle \tilde{\mathbf{q}}^*, \mathbf{L}\tilde{\mathbf{q}} \rangle,$$

  where $\tilde{\mathbf{q}}^*$ denotes the vector of adjoint disturbance variables.
- The PSE approach allows the analysis of a broader class of mean flows including those based on NS solvers.

[10] J.O. Pralits et al. "Optimal disturbances in three-dimensional boundary-layer flows". In: *Ercoftac Bull.* 74 (2007), pp. 23–31.

Non-linear development of optimal perturbations

- The linearly optimal disturbance is used as inflow condition with finite amplitude.
- The nonlinear-perturbation form of the parabolized Navier-Stokes equations are used, which is equivalent to the nonlinear plane-marching PSE[11] for a single stationary perturbation ($N = 0$, $\alpha_0 = 0$):

$$\tilde{\mathbf{q}}(x, y, z, t) = \sum_{n=-N}^{N} \hat{\mathbf{q}}_n(x, y, z) \exp\left[\mathrm{i} \int_x \alpha_n(x') dx' - \mathrm{i} n\omega t\right],$$

- An *implicit marching technique* is used to facilitate the computation of nonlinear streaks with large amplitudes.
- The instability of the resulting modified boundary layer flow is investigated by the linear form of the plane-marching PSE[12].

[11] P. Paredes et al. "The nonlinear PSE-3D concept for transition prediction in flows with a single slowly-varying spatial direction". In: *Procedia IUTAM* 14C (2015), pp. 35–44.

[12] P. Paredes. "Advances in global instability computations: from incompressible to hypersonic flow". PhD thesis. Universidad Politécnica de Madrid, 2014.

Verification: Optimal gain vs. spanwise wavenumber[13,14]

- Compressible, self-similar, flat plate boundary layer
- $Re_L = 10^8$ to enable comparison with asymptotic optimal growth results based on boundary layer equations

- $M = 10^{-3}$

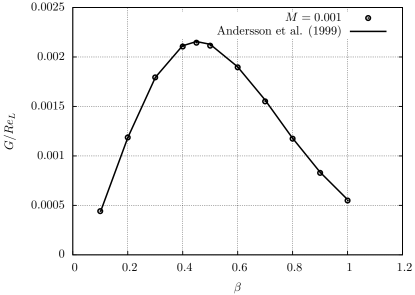

- $M = 3,\ T_0 = 333$ K

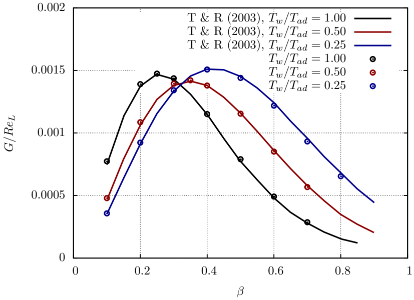

[13] P. Andersson, M. Berggren, and D.S. Henningson. "Optimal disturbances and bypass transition in boundary layers". In: *Phys. Fluids* 11 (1999), pp. 134–150.

[14] A. Tumin and E. Reshotko. "Optimal Disturbances in Compressible Boundary Layers". In: *AIAA J.* 41 (2003), pp. 2357–2363.

Self-similar vs. full Navier-Stokes solutions

- Optimal perturbations are commonly computed from the leading edge, $x_0 = 0$, using the self-similar base flow solution, which ignores both the viscous-inviscid interaction near the leading edge and the weak shock wave emanating from that region
- To assess the effects of this simplification, a realistic basic state based on the Navier-Stokes (NS) equations is used

- NS parameters: $R_n = 1\ \mu$m, $Re' = 10^6/$m, $T_0 = 333$ K, $T_w/T_{ad} = 1$

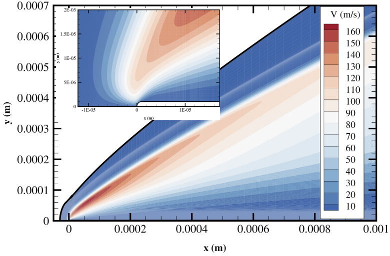

- Self-similar vs. NS b.l. profiles ($R = \sqrt{xU/\nu}$)

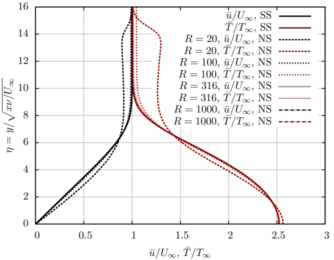

Effect of initial optimization position, x_0

- The final optimization position is $R_1 = \sqrt{x_1 U/\nu} = 1000$ with $x_1 = L = 1$ m, which is used as reference length

- Optimal gain using NS base flow
- Self-similar vs. NS results

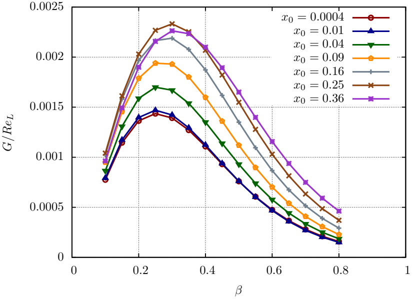

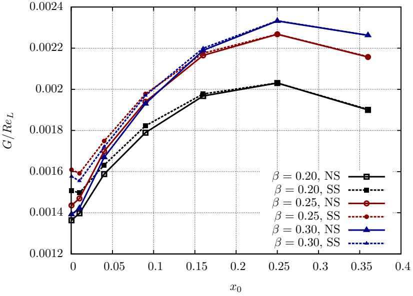

- Optimal $\beta = 0.25$ for inflow location at the leading edge
- The overall maximum G/Re_L is found for $x_0 = 0.25$ and $\beta = 0.30$
- As expected, the optimal G/Re_L results using self-similar and NS base flows agree for $x_0 > 0.25$, while there is up to 10% deviation for x_0 closer to the leading edge

Non-linear evolution of streaks initiated near $x_0 = 0$

- $R_0 = \sqrt{x_0 U/\nu} = 20$ and $\beta = 0.25$
- Initial amplitudes defined as $A_0 = \sqrt{E_0} = A/\sqrt{G_{max}}$ with $G_{max} = 2398$
- Streak amplitude based on u:
  $As_u(x) = [\max_{y,z}(\tilde{u}(x,y,z)) - \min_{y,z}(\tilde{u}(x,y,z))]/2$

- Streak amplitude, As_u

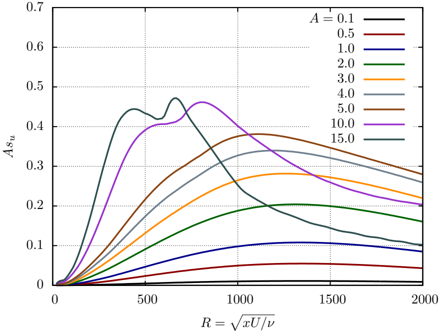

- Energy gain, $G = E/E_0$

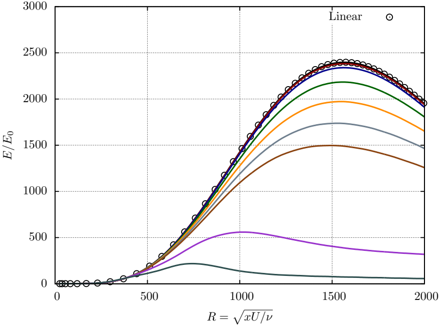

Structure of streaks during non-linear evolution

- Streak amplitude, As_u

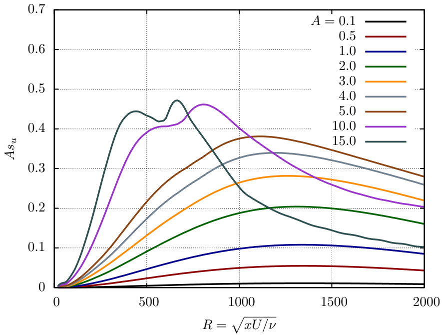

- $A = 3$
- $A = 10$

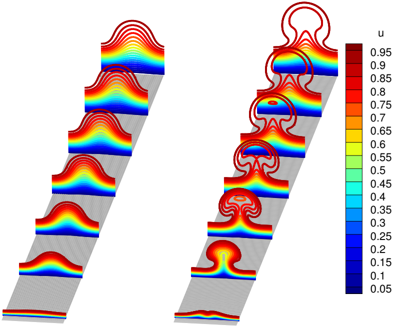

Non-linear streaks initiated at optimal x_0

- $R_0 = \sqrt{x_0 U/\nu} = 500$ and $\beta = 0.30$

- Streak amplitude, As_u

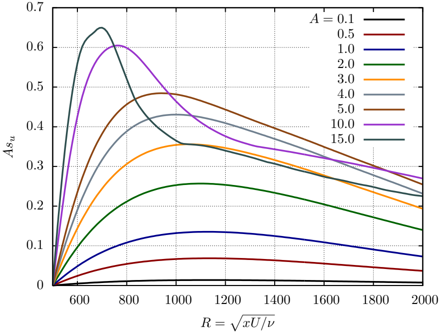

- Streak amplitude, As_u, for $x_0 \to 0$

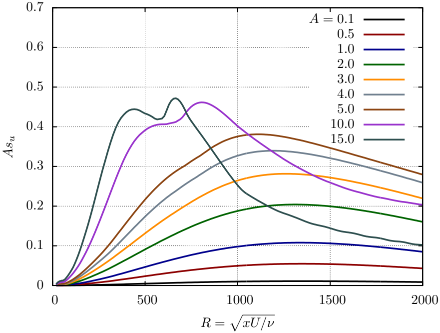

Structure of streaks initiated at optimal x_0 during non-linear evolution

- Streak amplitude, As_u

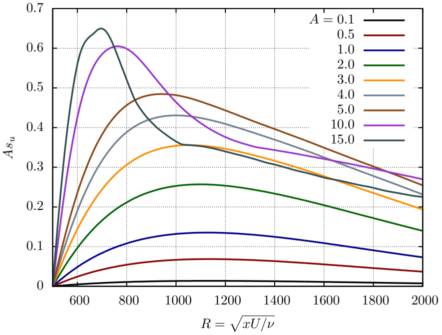

- $A = 3$
- $A = 10$

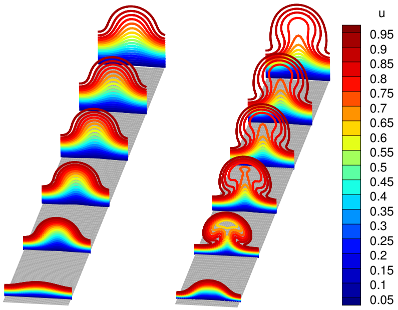

Instability of streaks initiated at the leading edge

- $R_0 = \sqrt{x_0 U/\nu} = 20$ and $\beta = 0.25$
- Spatial PDE based analysis at the final optimization position, $R_1 = 1000$
- Two types of shear layer modes become unstable, the sinuous (S) and the varicose (V) modes

- Growth rate, $-\alpha_i$, vs. frequency, ω

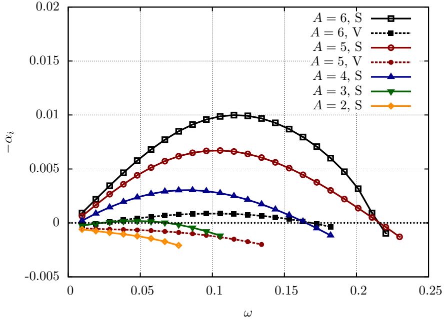

- Sinuous, $A = 6$, $\omega = 0.115$
- Varicose, $A = 6$, $\omega = 0.0958$

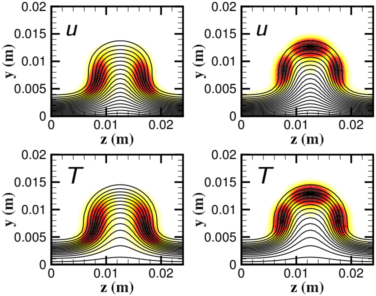

Amplitude evolution of streak instabilities

- $R_0 = \sqrt{x_0 U/\nu} = 20$ and $\beta = 0.25$
- Plane-marching PSE analysis of the sinuous mode
- N-factor based on Mack's energy norm

- $A = 3$

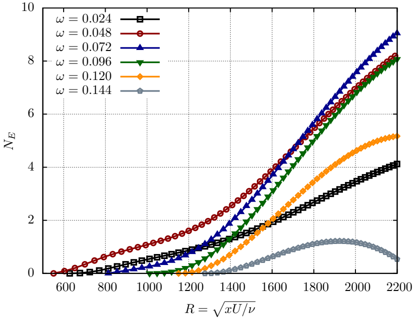

- $A = 5$

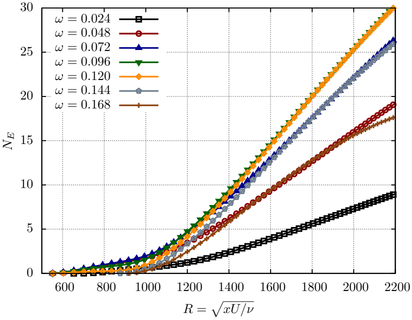

Natural transition in the unperturbed BL without streak

- Transition prediction based on $N_E = 9$ and 10
- Oblique first mode N_E computed by linear PSE

- N-factors based on E

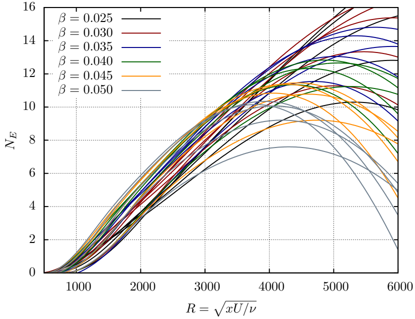

- Transition location, $Re_x = R^2$

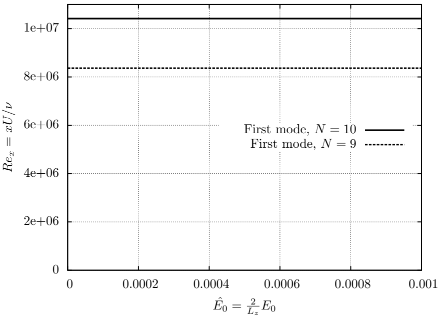

- $N = 10$: $Re_x = 1.0417 \times 10^7$, $\beta = 0.040$, $\omega \approx 0.012$
- $N = 9$: $Re_x = 8.3625 \times 10^6$, $\beta = 0.045$, $\omega \approx 0.012$

Bypass transition in a Mach 3 flat plate BL

- Transition prediction based on $N_E = 9$ and 10
- Sinuous mode N_E computed by linear plane-marching PSE

- As_u vs. $\hat{E}_0 = 2/L_z\, E_0$

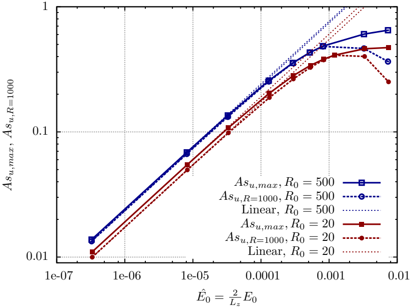

- Transition location, $Re_x = R^2$

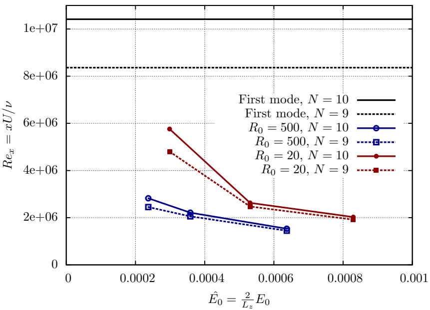

- $R_0 = 20$: $\beta = 0.25$, $\omega = 0.075 - 0.100$
- $R_0 = 500$: $\beta = 0.30$, $\omega = 0.075 - 0.100$
- Oblique first mode: $\beta = 0.040 - 0.045$, $\omega \approx 0.012$

- Verification of newly developed linear, adjoint-PSE based optimization code for compressible flows with results from literature.
- The effects of the viscous-inviscid interaction near the leading edge and the weak shock wave produce a 10% deviation from results based on self-similar base flow when the initial optimization position is located near the leading edge.
- Sinuous mode becomes unstable before the varicose mode for the moderate amplitude streaks studied.
- A non-linear perturbation form of the parabolized Navier-Stokes equations is demonstrated for the computation of the downstream development of high-amplitude stationary disturbances.
- The optimal initial optimization position for maximum energy also leads to earlier/stronger growth of secondary instability and, hence, earlier onset of bypass transition relative to other inflow locations.
- Bypass transition via finite-amplitude optimal disturbances is demonstrated for a zero-pressure-gradient flat plate boundary layer.

Instability of streaks initiated at the optimal x_0

- $R_0 = \sqrt{x_0 U/\nu} = 500$ and $\beta = 0.30$
- Spatial PDE based analysis at the final optimization position, $R_1 = 1000$
- Two types of shear layer modes become unstable, the sinuous (S) and the varicose (V) modes

- Growth rate, $-\alpha_i$, vs. frequency, ω

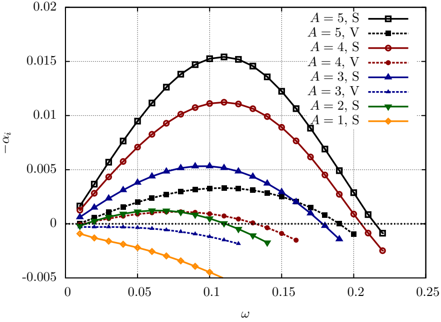

- Sinuous, $A = 5$, $\omega = 0.11$
- Varicose, $A = 5$, $\omega = 0.11$

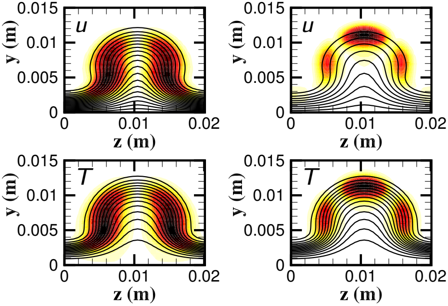

Amplitude evolution of streak instabilities

- $R_0 = \sqrt{x_0 U/\nu} = 500$ and $\beta = 0.30$
- Plane-marching PSE analysis of the sinuous mode along x
- N-factor based on Mack's energy norm

- $A = 2.7$

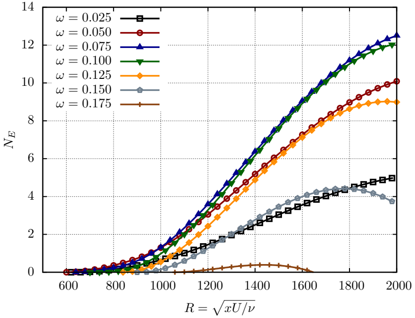

- $A = 4$